Deciphering Chemical Bonding in Golden Cages

Dmitry Yu. Zubarev and Alexander I. Boldyrev*

Department of Chemistry and Biochemistry, Utah State University, Logan, Utah 84322-0300

Received: September 11, 2008; Revised Manuscript Received: October 23, 2008

The recently developed adaptive natural density partitioning (AdNDP) method has been applied to a series of golden clusters. The pattern of chemical bonding in Au_{20} revealed by AdNDP shows that 20 electrons form a four-center−two-electron (4c−2e) bond in each of 10 tetrahedral cavities of the Au_{20} cluster. This chemical bonding picture can readily explain the tetrahedral structure of the Au_{20} cluster. Furthermore, we demonstrate that the recovered 4c−2e bonds corresponding to independent structural fragments of the cluster provide important information about *chemically* relevant fragmentation of Au_{20}. In fact, some of these bonds can be removed from the initial tetrahedral structure together with the associated atomic fragments, leading to the family of smaller gold clusters. Chemical bonding in the systems formed in such a manner is yet closely related to the bonding in the parental systems showing persistence of the 4c−2e bonding motif. Thus, the multicenter bonds in golden cages recovered by the AdNDP analysis correspond to the fragments that should be seen as building blocks of these chemical systems.

1. Introduction

Unique chemical and physical properties of nanoscale gold species[1−9] have stimulated research efforts in both experimental[10−21] and theoretical[22−36] fields. Considering the promise of these systems for the design of novel materials with tailored properties, molecular electronics, and nanocatalysts, the further growth of the efforts establishing structure/property relationships and providing a means of prediction of novel systems should be anticipated. The goal of the present study is to demonstrate that manipulations with structural subunits of the golden hollow cages derived from the tetrahedral Au_{20} cluster[11,14,18] (see Figure 1) can be easily related to the changes in the patterns of chemical bonding revealed by the recently developed adaptive natural density partitioning (AdNDP) method.[37] Thus, the AdNDP analysis can be used to detect chemically relevant structural fragments and produce a very simple and visual representation of chemical systems that can be related to their properties.

2. Theoretical Methods and Computational Details

The detailed description of the AdNDP algorithm can be found elsewhere.[37] In brief, this approach leads to partitioning of the charge density into elements with the lowest possible number of atomic centers per electron pair: *n*-center−two-electron (*n*c−2e) bonds, including core electrons, lone-pairs (LPs), 2c−2e bonds, etc. If some part of the density cannot be localized in this manner, it is represented using completely delocalized objects, similar to canonical MOs, naturally incorporating the idea of the completely delocalized bonding. Thus, AdNDP achieves a seamless description of different types of chemical bonds. The geometry optimization and normal-mode analysis for the studied systems were carried out using the hybrid density functional B3PW91[38] method with the LANL2DZ effective core potential and basis set[39] as implemented in the Gaussian 03 software package.[40] The density matrix in the basis of the natural atomic orbitals as well as the transformation between atomic orbital and natural atomic orbital basis sets was generated at the B3PW91/LANL2DZ level of theory by means of the NBO 3.1 code[41] incorporated into Gaussian 03. It is known that the results of the NBO analysis do not generally depend on the quality of the basis set, so the choice of the level of theory for the AdNDP analysis is adequate. The results of

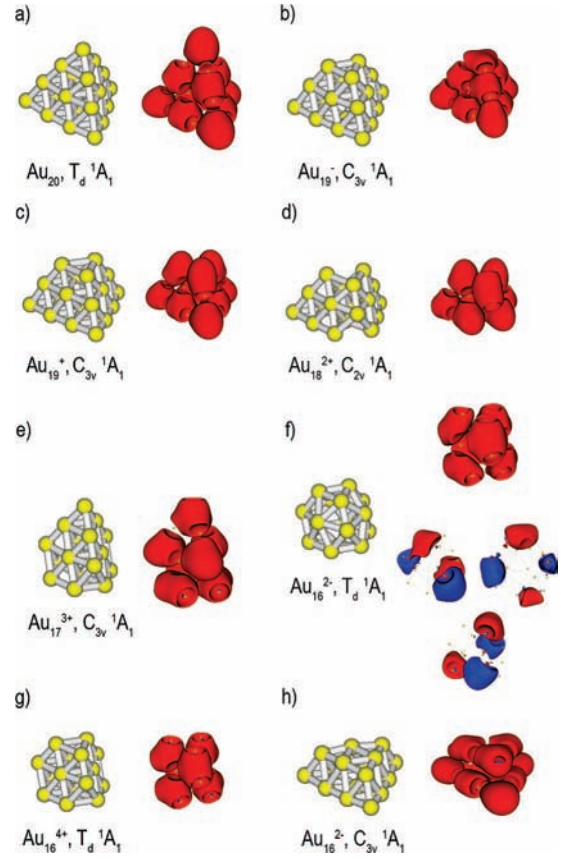

Figure 1. Structures of the gold clusters derived from the tetrahedral Au_{20} species and patterns of chemical bonding according to AdNDP.

* Corresponding author. E-mail: a.i.boldyrev@usu.edu.

10.1021/jp808103t CCC: $40.75
Published on Web 12/10/2008

the calculations are visualized using MOLEKEL 4.3[42] and MOLDEN 3.6.[43]

Some of the systems studied in the present paper are electronically unstable doubly charged anions. It has been demonstrated recently[44] that the instability toward the spontaneous detachment of an electron in such species leads to significant errors in the calculated physical properties if calculations are performed using compact basis sets and disregard scattering solutions. Nevertheless, it also has been demonstrated[45] that calculations of multiply charged anions with a compact basis set can provide reasonable chemical bonding models for the same anions stabilized in the external field, e.g., provided in the crystal structures by surrounding counterions. Thus, we believe that the reported bonding models for the doubly charged species are correct.

3. Results and Discussion

The tetrahedral Au_{20} golden cage (Figure 1a) discovered in molecular beams by Li et al.[11] is indeed a remarkable system. The chemical bonding model for this species was first conjectured by King et al.[25] It was proposed that 20 gold atoms retain their filled d^{10} shells while contributing one electron to the skeletal bonding each. These 20 electrons can be used to form a four-center−two-electron (4c−2e) bond in each of 10 tetrahedral cavities of the Au_{20} cluster. AdNDP is currently the only tool that can verify this heuristic prediction. The pattern of chemical bonding in Au_{20} revealed by AdNDP is presented in Figure 1a next to the structure of the Au_{20} cluster. Indeed, four 4c−2e bonds are found at the tetrahedral cavities at the vertices of the tetrahedral Au_{20} cage (occupation number ON_{vertex} = 1.72 |e|). Six more 4c−2e bonds are found in the tetrahedral cavities in the middle of the six edges of the tetrahedron (ON_{edge} = 1.98 |e|). Thus, results of the AdNDP analysis are in the perfect agreement with the conjecture made by King et al.[25]

Deciphered chemical bonding in the Au_{20}, T_d $^1A_1$ cluster is a valuable result by itself, since a very simple and assessable representation of the electronic structure of a three-dimensional cluster is provided on the basis of the analysis of the wave function. Yet, there is an even more important question to answer, namely, if the recovered 4c−2e bonds correspond to independent structural fragments of the cluster, or, in other words, does AdNDP provide information about *chemically* relevant fragmentation of the cluster?

The first step is to take away a Au^+ ion from one of the vertex positions of the tetrahedral Au_{20} unit producing Au_{19}^- anion (Figure 1b). This structure is the global minimum contributing to the photoelectron spectra obtained in molecular beams by Bulusu et al.[14] Since the amount of the electrons available for the skeletal bonding is not altered in this case, the bonding pattern in the experimentally observed Au_{19}^- C_{3v}, $^1A_1$ cluster[14] should be similar to the bonding pattern in Au_{20}, T_d $^1A_1$. The AdNDP analysis of Au_{19}^- shows nine 4c−2e bonds at the same positions as in Au_{20}, T_d $^1A_1$ (ON_{vertex} = 1.81 |e| and ON_{edge} = 1.60−1.98 |e|) and one 3c−2e bonds (ON = 1.91 |e|) at the face formed after the removal of the vertex of the tetrahedron (Figure 1b).

If the vertex Au atom is removed together with a pair of electrons, the Au_{19}^+, C_{3v} $^1A_1$ cation is formed (Figure 1c). It is not established if this particular structure is the global minimum on the potential energy surface, but it is indeed a local minimum. Thus, it is valid to perform the analysis of chemical bonding in this system and relate the results to the experimentally viable parental tetrahedral Au_{20} cluster. In the Au_{19}^+, C_{3v} $^1A_1$ species one should expect to find only nine skeletal bonds. According to the AdNDP results for the Au_{19}^+, C_{3v} $^1A_1$ cluster, these nine skeletal bonds involve the same fragments as in the Au_{20}, T_d $^1A_1$ and Au_{19}^- C_{3v}, $^1A_1$ clusters. There are three 4c−2e bonds at the vertices (ON_{vertex} = 1.71 |e|) and six 4c−2e bonds at the edges of the truncated tetrahedron (ON_{edge} = 1.84−1.96 |e|). The missing bond is the one associated with the removed vertex.

In the same manner, two vertices of the initial Au_{20}, T_d $^1A_1$ species can be removed together with two electron pairs, leading to the Au_{18}^{2+}, C_{2v} $^1A_1$ cluster (Figure 1d). This system is a local minimum on the corresponding potential energy surface. The bonding pattern revealed by AdNDP in this case clearly shows that the system is now short of two 4c−2e bonds associated with the removed atoms (Figure 1d). Two 4c−2e bonds are found at the remaining vertices (ON_{vertex} = 1.96 |e|) and six 4c−2e bonds at the edges (ON_{edge} = 1.53−1.92 |e|). All these bonds involve the same cluster fragments as in the systems considered above.

The local minimum structure of Au_{17}^{3+}, C_{3v} $^1A_1$ (Figure 1e), is obtained by cutting off three out of four vertices of the tetrahedral Au_{20} unit and taking away three electron pairs involved in the skeletal bonding. As the AdNDP analysis shows (Figure 1e), these three electron pairs are actually associated with the removed one-atomic fragments. Seven remaining electron pairs form seven 4c−2e bonds. One of them involves four atoms at the remaining vertex (ON_{vertex} = 1.95 |e|), and the other six involve tetrahedral fragments at the edges (ON_{edge} = 1.77−1.86 |e|). Indeed, the location of these skeletal bonds, if compared with the bonding pattern of Au_{20}, T_d $^1A_1$, is not affected by the removal of the three bonds at the truncated vertices. Though this structure has one imaginary frequency at the B3LYP/LANL2DZ level of theory, it is a true local minimum at the B3PW91/LANL2DZ level of theory. At both levels of theory the electronic configuration of the species is the same; thus, the reported results of the AdNDP analysis are valid.

It was demonstrated[14] that under the conditions of the photoelectron spectroscopic experiment the Au_{16}^- cluster is a tetrahedral unit, which is distorted because the system is an open shell. Its closed-shell counterpart is the Au_{16}^{2-}, T_d $^1A_1$ cluster shown at Figure 1f. This tetrahedral unit is in fact the truncated Au_{20}, T_d $^1A_1$ species. Comparison of the bonding patterns produced by AdNDP for these tetrahedral units shows that Au_{16}^{2-}, T_d $^1A_1$ preserves six 4c−2e bonds (ON_{edge} = 1.94 |e|) involving four-atomic fragments at the edges of the initial Au_{20}, T_d $^1A_1$ cluster. Also, three completely delocalized 16c−2e bonds are found (ON = 2.00 |e|) that are related to the triply degenerate t_2 highest occupied molecular orbital (HOMO) of Au_{16}^{2-}, T_d $^1A_1$. If the vertices of the Au_{20} are removed together with four electron pairs, the resulting Au_{16}^{4+}, T_d $^1A_1$ possesses only six localized 4c−2e bonds at the tetrahedron's edges with ON_{edge} = 1.85 |e| (Figure 1g).

Since the chemical bonds revealed in the above-discussed structures involve in general four-atomic fragments, it is logical to consider the Au_{16}^{2-}, C_{3v} $^1A_1$ cluster presented at Figure 1h, which is derived from the tetrahedral Au_{20}, T_d $^1A_1$ species by removing one electron pair together with the entire four-atomic fragment participating in a single 4c−2e bond at one of the vertices. The expected result of the AdNDP analysis would include nine multicenter bonds, three of which are located at the remaining vertices and six at the edges of the truncated tetrahedron. The bonding pattern revealed by AdNDP indeed supports this conjecture. There are three 3c−2e bonds located at the face formed after the tetrahedron truncation (ON_{edge} = 1.97 |e|). These bonds are residues of three 4c−2e bonds at the

tetrahedron's edges that lost one atom each. Three 4c−2e bonds at the preserved edges have the same appearance as in the Au_{20}, T_d $^1A_1$ cluster (ON_{edge} = 1.91 |e|). Finally, three 3c−2e bonds are found at the remaining vertices (ON_{vertex} = 1.70 |e|). This is the most noticeable alternation in the bonding picture, since analogous bonds in Au_{20}, T_d $^1A_1$ involve four-atomic fragments. The observed transition from 4c−2e to 3c−2e bonds should be connected to the distortion of the geometry of the cluster, which now can be seen as consisting of two atomic layers, rather than being a hollow cage.

The present study shows that indeed the multicenter bonds recovered by the AdNDP analysis correspond to the fragments that should be seen as building blocks of chemical systems. Thus, *n*c−2e bonds provide information about chemically relevant fragmentation in the particular species. We believe that it can be used further to establish simple and efficient relationships between structure and properties.

Acknowledgment. This work was supported by the National Science Foundation (CHE-0714851).

Supporting Information Available: Optimized Cartesian coordinates and normal modes for the analyzed species. This material is available free of charge via the Internet at http://pubs.acs.org.

References and Notes

(1) Haruta, M.; Yamada, N.; Kobayashi, T.; Iijima, S. *J. Catal.* **1989**, *115*, 301.
(2) Haruta, M.; Tsubota, S.; Kobayashi, T.; Kageyama, H.; Genet, M. J.; Delmon, B. *J. Catal.* **1993**, *144*, 175.
(3) Elghanian, R.; Storhoff, J. J.; Mucic, R. C.; Letsinger, R. L.; Mirkin, C. A. *Science* **1997**, *277*, 1078.
(4) Valden, M.; Lai, X.; Goodman, D. W. *Science* **1998**, *281*, 1647.
(5) Heiz, U.; Schneider, W. D. *J. Phys. D: Appl. Phys.* **2000**, *33*, R85.
(6) Lopez, N.; Norskov, J. K. *J. Am. Chem. Soc.* **2002**, *124*, 11262.
(7) Boyen, H. G.; Kastle, G.; Weigl, F.; Koslowski, B.; Dietrich, C.; iemann, P.; Spatz, J. P.; Riethmuller, S.; Hartmann, C.; Moller, M.; Schmid, G.; Garnier, M. G.; Oelhafen, P. *Science* **2002**, *297*, 1533.
(8) Haruta, M. *Sci. Technol. Catal. 2002* **2003**, *145*, 31.
(9) Daniel, M. C.; Astruc, D. *Chem. Rev.* **2004**, *104*, 93.
(10) Furche, F.; Ahlrichs, R.; Weis, P.; Jacob, C.; Gilb, S.; Bierweiler, T.; Kappes, M. *J. Chem. Phys.* **2002**, *117*, 6982.
(11) Li, J.; Li, X.; Zhai, H. J.; Wang, L. S. *Science* **2003**, *299*, 864.
(12) Hakkinen, H.; Yoon, B.; Landman, U.; Li, X.; Zhai, H. J.; Wang, L. S. *J. Phys. Chem. A* **2003**, *107*, 6168.
(13) Zhai, H. J.; Kiran, B.; Dai, B.; Li, J.; Wang, L. S. *J. Am. Chem. Soc.* **2005**, *127*, 12098.
(14) Bulusu, S.; Li, X.; Wang, L. S.; Zeng, X. C. *Proc. Natl. Acad. Sci. U.S.A.* **2006**, *103*, 8326.
(15) Wang, L. M.; Bulusu, S.; Huang, W.; Pal, R.; Wang, L. S.; Zeng, X. C. *J. Am. Chem. Soc.* **2007**, *129*, 15136.
(16) Jadzinsky, P. D.; Calero, G.; Ackerson, C. J.; Bushnell, D. A.; Kornberg, R. D. *Science* **2007**, *318*, 430.
(17) Heaven, M. W.; Dass, A.; White, P. S.; Holt, K. M.; Murray, R. W. *J. Am. Chem. Soc.* **2008**, *130*, 3754.
(18) Gruene, P.; Rayner, D. M.; Redlich, B.; van der Meer, A. F. G.; Lyon, J. T.; Meijer, G.; Fielicke, A. *Science* **2008**, *321*, 674.
(19) Toikkanen, O.; Ruiz, V.; Ronnholm, G.; Kalkkinen, N.; Liljeroth, P.; Quinn, B. M *J. Am. Chem. Soc.* **2008**, *130*, 11049 DOI: 10.1021/ja802317t.
(20) Koshevoy, I. O.; Koskinen, L.; Haukka, M.; Tunik, S. P.; Serdobintsev, P. Yu.; Melnikov, A. S.; Pakkanen, T. A. *Angew. Chem., Int. Ed.* **2008**, *47*, 3942 DOI: 10.1002/anie200800452.
(21) Femoni, C.; Iapalucci, M. C.; Longoni, G.; Tiozzo, C.; Zacchini, S.; *Angew. Chem., Int. Ed.* **2008**, *47*, 6666 DOI: 10.1002/anie.200802267.
(22) King, R. B. *Inorg. Chim. Acta* **1986**, *116*, 109.
(23) Garzon, I. L.; Michaelian, K.; Beltran, M. L.; Posada-Amarillas, A.; Ordejon, P.; Artacho, E.; Sanchez-Portal, D.; Soler, J. M. *Phys. Rev. Lett.* **1998**, *81*, 1600.
(24) King, R. B. *Inorg. Chim. Acta* **1998**, *277*, 202.
(25) King, R. B.; Chen, Z.; Schleyer, P. v. R. *Inorg. Chem.* **2004**, *43*, 4564.
(26) Xiao, L.; Wang, L. C. *Chem. Phys. Lett.* **2004**, *392*, 452.
(27) Gu, X.; Ji, M.; Wei, S. H.; Gong, X. G. *Phys. Rev. B* **2004**, *70*, 205401.
(28) Fa, W.; Luo, C. F.; Dong, J. M. *Phys. Rev. B* **2005**, *72*, 205428.
(29) Wang, J.; Jellinek, J.; Zhao, J.; Chen, Z.; King, R. B.; Schleyer, P. v. R. *J. Phys. Chem. A* **2005**, *109*, 9265.
(30) Walter, M.; Hakkinen, H. *Phys. Chem. Chem. Phys.* **2006**, *8*, 5407.
(31) Bulusu, S.; Zeng, X. C. *J. Chem. Phys.* **2006**, *125*, 154303.
(32) Sun, Q.; Wang, Q.; Chen, G.; Jena, P. *J. Chem. Phys.* **2007**, *127*, 214706.
(33) Krishnamurty, S.; Shafai, G. S.; Kanhere, D. G.; Soule de Bas, B.; Ford, M. J. *J. Phys. Chem. A* **2007**, *111*, 10769.
(34) Tian, D.; Zhao, J. *J. Phys. Chem. A* **2008**, *112*, 3141.
(35) Torres, M. B.; Fernandez, E. M.; Balbas, L. C. *J. Phys. Chem. A* **2008**, *112*, 6678.
(36) Jiang, D.; Tiago, M. L.; Luo, W.; Dai, S. *J. Am. Chem. Soc.* **2008**, *130*, 2777.
(37) Zubarev, D. Yu.; Boldyrev, A. I. *Phys. Chem. Chem. Phys.* **2008**, *10*, 5207.
(38) (a) Becke, A. D. *J. Chem. Phys.* **1993**, *98*, 5648. (b) Burke, K.; Perdew, J. P.; Wang, Y. In *Electronic Density Functional Theory: Recent Progress and New Directions*; Dobson, J. F., Vignale, G., Das, M. P., Eds.; Plenum, New York, 1998.
(39) (a) Hay, P. J.; Wadt, W. R. *J. Chem. Phys.* **1985**, *82*, 270. (b) Wadt, W. R.; Hay, P. J. *J. Chem. Phys.* **1985**, *82*, 284. (c) Hay, P. J.; Wadt, W. R. *J. Chem. Phys.* **1985**, *82*, 299.
(40) Frisch, M. J.; et al. Gaussian 03, revision A.1; Gaussian, Inc.: Pittsburgh, PA, 2003.
(41) Glendening, E. D.; Reed, A. E.; Carpenter, J. E.; Weinhold, F. NBO 3.1.
(42) Portmann, S. MOLEKEL, version 4.3.; CSCS/ETHZ, 2002.
(43) Schaftenaar, G. MOLDEN 3.4; CAOS/CAMM Center, The Netherlands, 1998.
(44) Lambrecht, D. S.; Fleig, T.; Sommerfeld, T. *J. Phys. Chem. A* **2008**, *112*, 2855.
(45) Zubarev, D. Yu.; Boldyrev, A. I. *J. Phys. Chem. A* **2008**, *112*, 7984.

JP808103T